

# Ionophore-mediated swelling of erythrocytes as a therapeutic mechanism in sickle cell disease

Athena C. Geisness<sup>1,\*</sup>, Melissa Azul<sup>1,2\*</sup>, Dillon Williams<sup>1</sup>, Hannah Szafraniec<sup>1</sup>,  
Daniel C. De Souza<sup>3,4,5</sup>, John M. Higgins<sup>3,4,5</sup> and David K. Wood<sup>1</sup>

<sup>1</sup>Department of Biomedical Engineering, University of Minnesota Twin Cities, Minneapolis, MN; <sup>2</sup>Department of Pediatric and Adolescent Medicine, Division of Pediatric Hematology-Oncology, Mayo Clinic, Rochester, MN; <sup>3</sup>Department of Systems Biology, Harvard Medical School, Boston, MA; <sup>4</sup>Department of Pathology, Massachusetts General Hospital, Harvard Medical School, Boston, MA and <sup>5</sup>Center for Systems Biology, Massachusetts General Hospital, Harvard Medical School, Boston, MA, USA

*\*ACG and MA contributed equally as co-first authors.*

## Correspondence:

David K. Wood  
[dkwood@umn.edu](mailto:dkwood@umn.edu)

**Received:** March 8, 2021.

**Accepted:** October 18, 2021.

**Pre published:** October 28, 2021.

<https://doi.org/10.3324/haematol.2021.278666>

©2022 Ferrata Storti Foundation

Haematologica material is under a license CC

BY-NC 

## **Supplementary to Ionophore-mediated swelling of erythrocytes as a therapeutic mechanism in sickle cell disease (*Effect of osmotic swelling on sickle erythrocytes*)**

### **Supplemental Methods**

#### *Patient Sample Collection*

Blood samples were collected from patients with SCD or healthy volunteers for AA controls during routine clinic visits in accordance with protocol 2006P000066/PHS and STUDY0000003, approved by the University of Minnesota Medical Center Institutional Review Board (IRB). Baseline laboratory measurements displayed in table 1 and supplementary table 1 were obtained in the clinic on the day of sample collection and values were provided by patients' medical providers. Blood samples were collected and stored at 4°C in sodium citrate blood collection tubes. Additional samples (n=3) used for morphology experiments were collected from patients with SCD and stored in ethylenediaminetetraacetic acid (EDTA). Samples were stored up to 5 days prior to treatment or experimentation.

#### *Hematologic Parameter Analysis*

After monensin treatment, the sample's complete blood count (CBC) was analyzed using a Sysmex XS-1000i hematology analyzer, by the Advanced Research and Diagnostic Laboratory (ARDL) at the University of Minnesota. Monensin effect on osmotic swelling and intracellular water content was quantified by measuring MCHC and MCV.

#### *Device Design and Fabrication*

Once samples were prepared and hematologic measurements made, samples were perfused through a microfluidic device. The construction of similar devices has been described previously<sup>1-3</sup>. The device is comprised of three polydimethylsiloxane (PDMS) (Sylgard 184, Dow Corning) layers: a blood channel, hydration, and gas layer, shown in supplemental figure 1. Each layer was designed to serve an intended function. The blood layer contains a channel which splits into a bypass and observation channel each measuring 15µm x 15µm with a length of 10mm (Figure S1a). These dimensions approximate the physiological diameter of some post-capillary venules within the microvasculature. The bypass channel was used to maintain flow to prevent packing of RBCs in the observation channel during potential occlusions. Stacked over the blood layer (Figure S1d) is a 100µm tall hydration layer (Figure S1c), where PBS is perfused to prevent dehydration of the RBCs during experimentation. The gas channel (Figure S1b) is 150µm in height and lies on top of the previously described two layers. The oxygen permeability of PDMS in this device has been previously reported<sup>3</sup>. Each layer is separated by a 100 µm PDMS membrane.

Device fabrication involves photolithography techniques and use of negative photoresist (SU8, MicroChem) to create a silicon wafer master mold for each layer, as described in a previous publication<sup>2</sup>. After developing the photoresist, wafers were salinized (448931-10G, Sigma-Aldrich) to decrease adhesion of the PDMS to the wafer. Each layer was then made by casting PDMS at an elastomer/curing agent ratio of 10:1 onto each master mold. For the gas layer, PDMS was cast onto the master mold to achieve a thickness of approximately 5mm. For the blood and hydration layers, previously described PDMS compression molding technique created each layer's individual thickness<sup>1-3</sup>. The PDMS layers were cured at 75°C for 2hrs. Inlets and outlets of the device were created using 20-gauge punches. A plasma cleaner was used to covalently bond each layer together by exposing PDMS surfaces for 2 minutes at a power of

100W. The entire device was then plasma bonded to a microscope glass slide. After plasma treatment, the devices were dehydrated to ensure secure bonding by placing them on a hotplate for 15 minutes.

### *Experimental Setup*

Microfluidic devices were mounted on a temperature regulated (37°C) Zeiss Axio Observer microscope. Specific oxygen tensions were selected and perfused through the gas layer using a solenoid board and gas mixing system that mixed 160mmHg oxygen gas (21% O<sub>2</sub>, 5% CO<sub>2</sub>, balance N<sub>2</sub>) with 0mmHg oxygen gas (5% CO<sub>2</sub>, balance N<sub>2</sub>). The partial pressure of 160mmHg oxygen is used to replicate ambient oxygen tension. While the physiologic oxygen tension of the venous circulation is 30-40mmHg, 0mmHg is used to demonstrate extreme hypoxic conditions to observe maximum sRBC sickling effect. The gas channel that overlays the bypass channel remained at 160mmHg oxygen, while the gas channel overlaying the observation channel was cycled between 160mmHg and 0mmHg oxygen at 3-5min intervals until a steady state (SS) velocity was reached for 1 minute of SS data collection. SS velocity for each oxygen cycle is defined by the period over which the maximum difference within the velocity values is less than two standard deviations from the average. At the outlet of the observation and bypass channel gas ports, a fiber optic oxygen sensor (NeoFox-GT, Ocean Optics) was used to continuously monitor oxygen tensions throughout the experiment. PBS was perfused through the hydration layer by a syringe pump (NE-500, New Era Pump Systems) at 500µm/s, to prevent sRBC dehydration. A pressure regulator (PCD-15PSIG, Alicat Scientific) set to a constant PSI perfused the blood through the device to achieve an initial velocity of 700µm/s at normoxia, corresponding to a physiologically relevant venule shear rate of 373s<sup>-1</sup>.

### *Quantitative Absorptive Cytometry*

Quantitative Absorptive Cytometry (QAC) platform was used as an assay to detect polymer content and morphological changes induced by monensin-treatment. Three additional samples from SCD patients were obtained using methods listed above. The hematological data from these samples are listed in table 1 of this supplement. QAC builds off previous work published by Di Caprio et al<sup>4</sup> to quantify morphology of RBCs in high throughput manner under variable oxygen tension. The optical absorption properties of oxygenated and deoxygenated hemoglobin are leveraged to quantify the ratio of the two species. Single cell images are recorded to calculate saturation from the ratio of oxy and dexoyhemoglobin, and the morphology of the cells is analyzed by a convolution neural net to determine if the cells contain detectable levels of polymer or if all hemoglobin is soluble.

QAC uses a previously developed microfluidic device in the Di Caprio study<sup>4</sup>. This device consists of a blood layer with a 30mm straight channel and a 25mm diffusion section. There is a 5mm imaging section. The diffusion section has a matrix of pillars to disperse the cells and is sufficiently long for the cells to reach steady state saturation. The imaging section has 21, 30µm channels to image individual cells. The gas layer on this device is a snaked channel that overlays the diffusion and imaging section.

Samples are prepared with a washing step; 50 ul of the blood sample is added to 200ul of PBS and spun at 2000 rpm for 2 minutes. A solution of 288 ul of 25 percent 7.4 pH albumin and 12 µl of 20 percent w/v acid blue 9 is added to 10 µL of the pellet to achieve a hematocrit of 3%. In table S1, the hematologic parameters prior to resuspension are shown. Albumin is used for

this experiment to match the refractive index of the red cells as this is necessary for accurate measuring of light attenuation.

The optical set up for QAC also builds off of Di Caprio's work. The main principle is red cells are illuminated with alternating blue LEDs in the Soret band and a constant red LED. In the Soret Band oxygenated hemoglobin has a peak absorption at 410nm and deoxygenated hemoglobin has a peak absorption at 430nm. By alternating these two LEDs and capturing images of the same cell at both wavelengths the mass of oxy and deoxyhemoglobin is recorded and the cell saturation is calculated using each species' known extinction coefficient. The constant red LED is used to calculate cell volume. The camera captures images in Bayer RGB matrix with no color processing, thus the blue pixels of the matrix alternate between the two blue LEDs and the red pixels capture the constant red light.

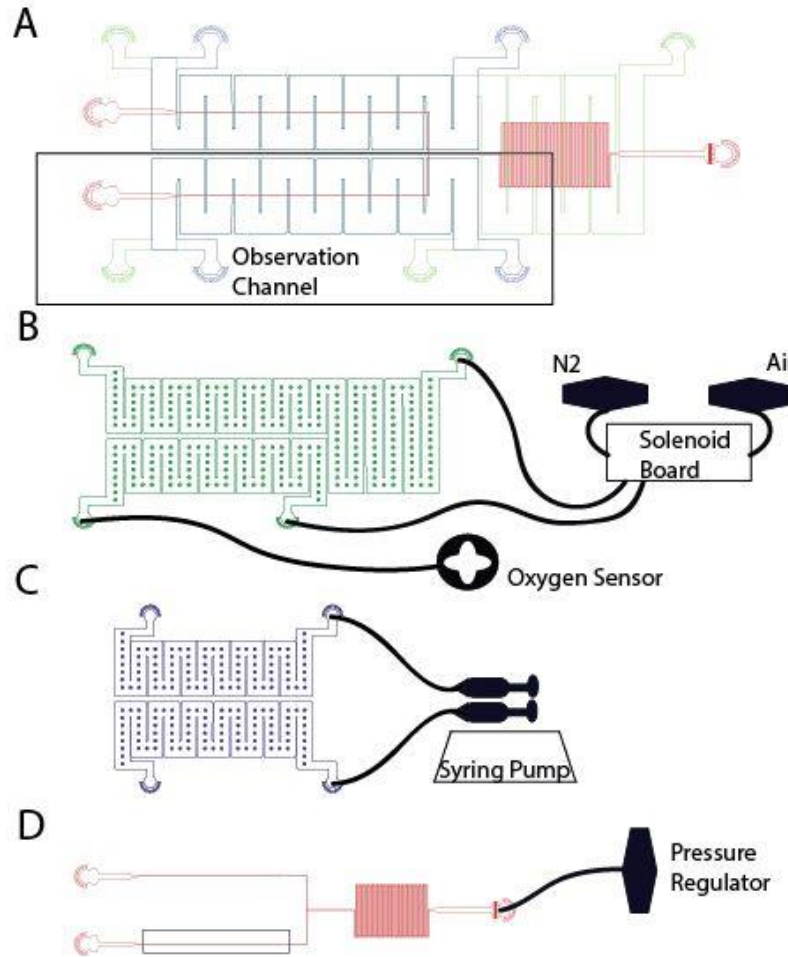
Images are captured at a rate of 200fps with each blue LED triggering at 100 fps. Raw images are converted to uint8 matrices and are separated by red and blue color channels and resized using MATLAB. A MATLAB script tracks cells and records the intensity of each cell at 410nm and 430 nm then takes the ratio to calculate cell saturation. The cell images for the two blue LED frames and the red LED frame are combined and the morphology is analyzed by a ResNet 50 neural net to classify the cell's hemoglobin as soluble or polymerized.

Data collection proceeds as follows: flow is stabilized for 10 min at 160 mmHg oxygen tension. After the settling time, 500 frame segments are captured, and the cell saturation is calculated. This is done several times to ensure the cells have reached steady state saturation. When steady state is reached 15000 frames are captured. This is repeated for 0, 15, 30, 45, 60, and 90 mmHg oxygen tensions with 10 minutes between the 160 mmHg and 0 mmHg step and 5 minutes between the rest.

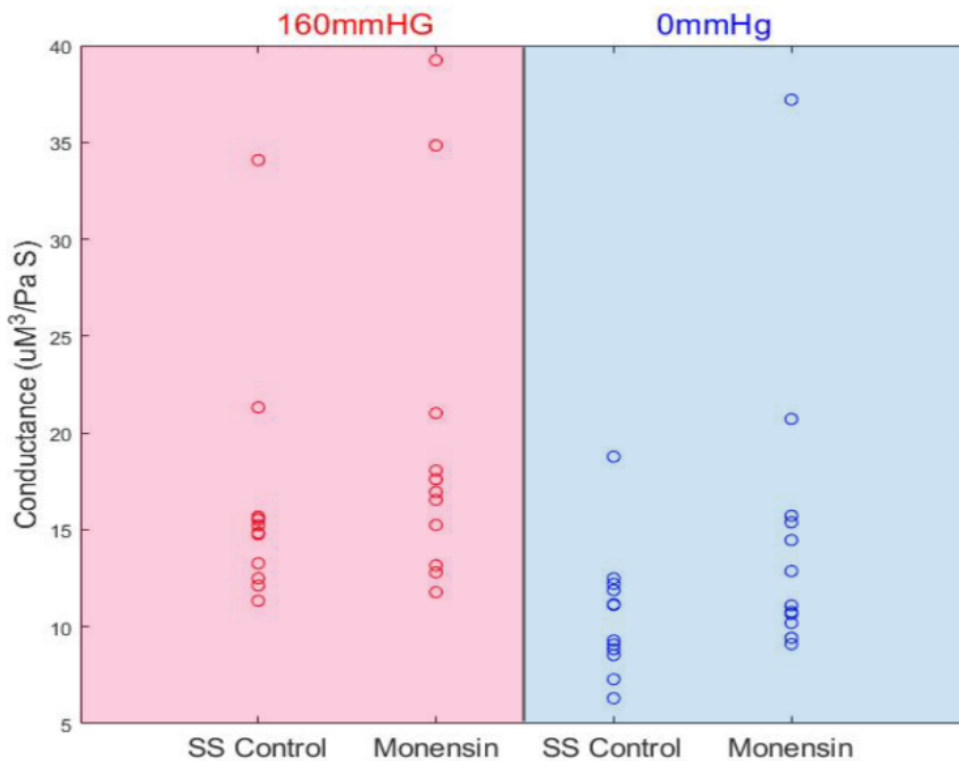
## References

1. Wood DK, Soriano A, Mahadevan L, Higgins JM, Bhatia SN. A biophysical indicator of vaso-occlusive risk in sickle cell disease. *Sci Transl Med*. 2012, 4(123).
2. Lu X, Wood DK, Higgins JM. Deoxygenation Reduces Sickle Cell Blood Flow at Arterial Oxygen Tension. *Biophys J*. 2016 110(12), 2751-2758.
3. Valdez JM, Datta YH, Higgins JM, and Wood DK. A microfluidic platform for simultaneous quantification of oxygen-dependent viscosity and shear thinning in sickle cell blood. *APL Bioeng*. 2019, 3(4) 046102.
4. Di Caprio G, Schonbrun E, Goncalves BP, Valdez JM, Wood DK, Higgins JM. High-throughput assessment of hemoglobin polymer in single red blood cells from sickle cell patients under controlled oxygen tension. *Proc Natl Acad Sci USA*. 2019;116(50):25236-25242.

## Supplemental Figures

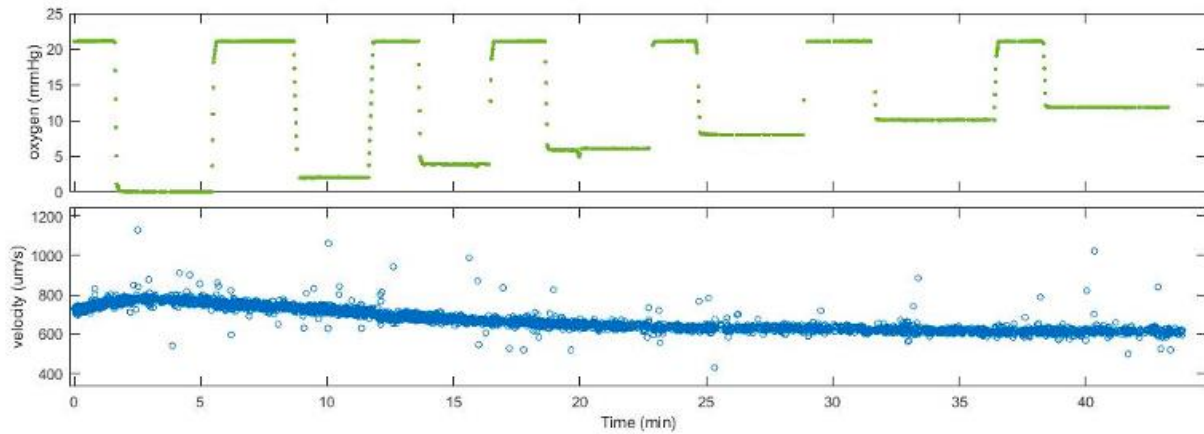


**S1: Device design and setup.** Schematic of microfluidic device used in rheology experiments. (a) The blood channel (red) is split into two venule sized channels: bypass and observation. The middle and top layers contain the hydration channels (blue) and gas channels (green) that separate and overlay the bypass and observation channels in the blood layer distinctly. This enables independent control of oxygen tensions in each bypass and observation channel. The device was designed to overlay each layer with the layer below to enable vertical diffusion of oxygen through the device to the blood channel and prevent the transport of oxygen between the bypass and observation channels. Each layer is accessed using inlet and outlet ports. (b) A solenoid valve attached to compressed gas cylinders containing 95% N<sub>2</sub> and 95% air balanced with CO<sub>2</sub> were used to control the oxygen tension supplied to the bypass and observation channels. An oxygen sensor, at the outlet of the gas layer's observation channel, was used to measure the oxygen tension inside the device. (c) PBS is perfused through both hydration channels by a double syringe pump. (d) A pressure regulator connected to the inlet of the blood channel was used to perfuse the blood at the desired oxygenated velocity. Data was collected using a highspeed camera to image a section of the observation channel.

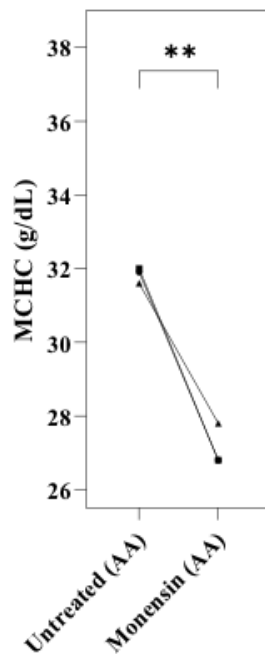
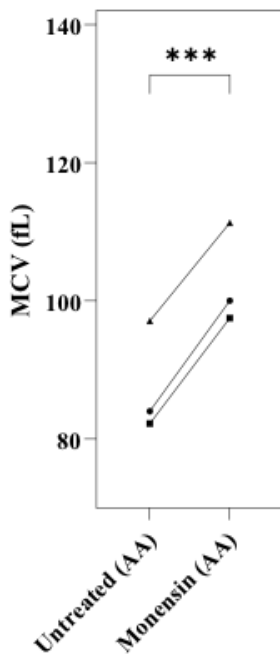


**S2: Experimental conductance.** The conductance of untreated controls and monensin-treated samples under oxygenated (160mmHg) and deoxygenated (0mmHg) conditions. A Wilcoxon signed-rank test was used to determine if there is a significant difference between the control group and monensin treatment. Conductance was calculated using the blood flow rate and driving pressure. There was no significant difference between the control and monensin group during oxygenation, however there was a significant difference under deoxygenation ( $p < 0.05$ ,  $n=13$ ). This indicates differences in initial oxygenated velocities is negligible due to its dependence on the driving pressure and that differences in deoxygenated velocities are not due to differences in the initial velocities. The higher conductance points observed in normoxia in this figure correspond to MCV values of 91.8 fL and 98.3 fL and are within the lower quartile of MCV values within this study.

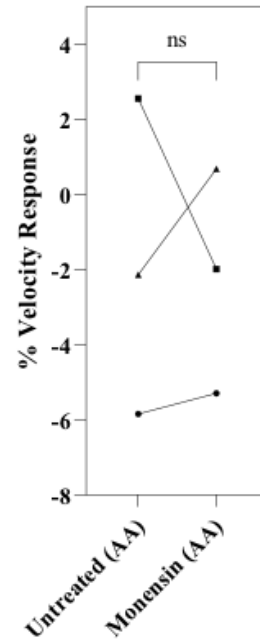
A



B



C

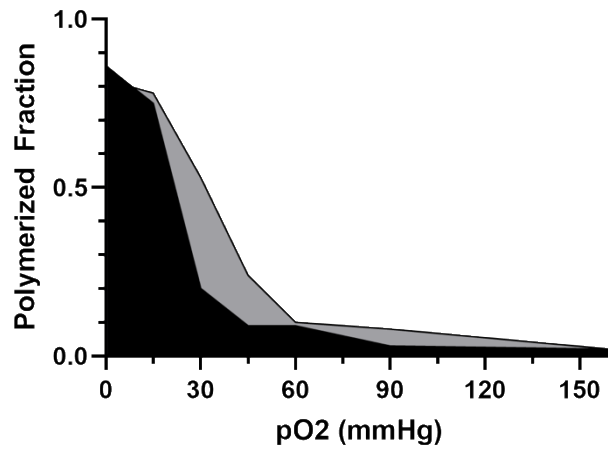


**S3: AA controls.** (a) Representative image of raw velocity data from a single AA patient sample. Oxygen tension (%) is displayed above in green and velocity ( $\mu\text{m}/\text{sec}$ ) displayed in blue. Despite various oxygen tensions, there is no velocity response, demonstrating oxygen-independent velocity. This is in contrast to oxygen-dependent velocity response seen in sickle samples (Figure 1b). Similar responses were seen when repeated with 2 additional AA samples tested. (b) Monensin effect on MCV and MCHC in healthy AA blood. There were significant increases in MCV ( $p=0.001$ ) and decreases in MCHC ( $p=0.009$ ) with monensin treatment. Similar increases in MCV and decreases MCHC were seen in SCD patient samples (Figure 3a-

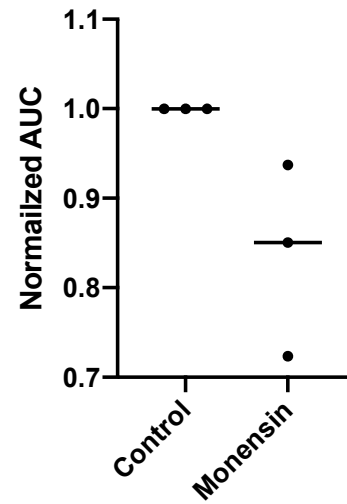


3b). (c) Summary of velocity response of 3 AA blood samples in the untreated and monensin-treated conditions. There was no significant change in velocity response between treatment and control conditions when exposed to hypoxia ( $p=0.874$ ). A two-tailed paired t-test was used to determine significance between untreated and monensin-treated groups in all comparisons.

A



B



**S4. RBC morphology analysis.** A) Representative data from one SCD patient sample depicting the fraction of polymerized cells as a function of oxygen tension with monensin treatment (black) compared to untreated (gray) using QAC methodology. A lower fraction of polymerized cells is seen in this sample with monensin treatment compared to untreated, with greatest differences emerging around 30mmHg. (B) Similar curves to (A) were generated for two additional SCD samples and the AUC between monensin-treated and their untreated controls were measured and compared. AUC's were normalized to the untreated control. Although monensin-treated samples had smaller AUC's signifying a lower polymerized fraction, sample response varied and the difference was non-significant using a paired two-tailed t-test (1.00 vs 0.84,  $p=0.12$ ).

Table S1. Hematological parameters of samples (HbSS) used in QAC

	<b>Condition</b>	<b>WBC</b> (x10 <sup>3</sup> /μL)	<b>RBC</b> (x10 <sup>6</sup> /μL)	<b>HGB</b> (g/dL)	<b>HCT</b> (%)	<b>MCV</b> (fL)	<b>MCH</b> (pg)	<b>MCHC</b> (g/dL)	<b>PLT</b> (x10 <sup>3</sup> /μL)
<b>1</b>	Whole Blood	14.8		9.2	26.7	85		34.5	
	Ethanol control	1.2	0.77	2.1	6.6	85.7	27.3	31.8	5
	10 nM Monensin	0.6	0.72	2.1	6.8	94.4	29.2	30.9	0
<b>2</b>	Whole Blood								
	Ethanol control	3.8	0.87	2.8	7.7	88.5	32.2	36.4	0
	10 nM Monensin	4.3	0.99	3.1	9.2	92.9	31.3	33.7	1
<b>3</b>	Whole Blood	8.92			22.8	110.7		33.8	
	Ethanol Control	0.2	0.5	1.7	5.5	110	34	30.9	0
	10 nM Monensin	0.9	1.62	5.8	20.9	129	35.8	27.8	8